HAL
open science

NDT-based design of joint material for the detection of bonding defects by infrared thermography

Matthias Barus, Hélène Welemane, Valérie Nassiet, Marie-Laetitia Pastor, Arthur Cantarel, Francis Collombet, Laurent Crouzeix, Yves-Henri Grunevald

To cite this version:

Matthias Barus, Hélène Welemane, Valérie Nassiet, Marie-Laetitia Pastor, Arthur Cantarel, et al.. NDT-based design of joint material for the detection of bonding defects by infrared thermography. NDT & E International, 2018, 93, pp.157-163. 10.1016/j.ndteint.2017.10.005 . hal-01758594

HAL Id: hal-01758594

https://hal.science/hal-01758594v1

Submitted on 4 Apr 2018

HAL is a multi-disciplinary open access archive for the deposit and dissemination of scientific research documents, whether they are published or not. The documents may come from teaching and research institutions in France or abroad, or from public or private research centers.

L'archive ouverte pluridisciplinaire **HAL**, est destinée au dépôt et à la diffusion de documents scientifiques de niveau recherche, publiés ou non, émanant des établissements d'enseignement et de recherche français ou étrangers, des laboratoires publics ou privés.

Open Archive Toulouse Archive Ouverte (OATAO)
OATAO is an open access repository that collects the work of Toulouse researchers and makes it freely available over the web where possible.

This is an author-deposited version published in: http://oatao.univ-toulouse.fr/
Eprints ID: 19551

To link to this article: DOI:10.1016/j.ndteint.2017.10.005
URL : https://doi.org/10.1016/j.ndteint.2017.10.005

To cite this version:

Barus, Matthias and Welemane, Hélène and Nassiet, Valérie and Pastor, Marie-Laetitia and Cantarel, Arthur and Collombet, Francis and Crouzeix, Laurent and Grunevald, Yves-Henri *NDT-based design of joint material for the detection of bonding defects by infrared thermography.* (2018) NDT&E International, vol. 93. pp. 157-163. ISSN 0963-8695

Any correspondence concerning this service should be sent to the repository administrator: staff-oatao@listes-diff.inp-toulouse.fr

NDT-based design of joint material for the detection of bonding defects by infrared thermography

M. Barus [a,b], H. Welemane [b,*], V. Nassiet [b], M.L. Pastor [c], A. Cantarel [c], F. Collombet [a], L. Crouzeix [a], Y.H. Grunevald [d]

[a] *Institut Clément Ader (ICA), Univ. de Toulouse, CNRS, UT3, Toulouse, France*
[b] *Laboratoire Génie de Production (LGP), INP-ENIT, Univ. de Toulouse, Tarbes, France*
[c] *Institut Clément Ader (ICA), Univ. de Toulouse, CNRS, UT3, IUT de Tarbes, France*
[d] *Composites Expertise & Solutions (CES), Castanet Tolosan, France*

A B S T R A C T

Non Destructive Testing (NDT) by active InfraRed Thermography (IRT) of bonded Carbon Fibers Reinforced Plastic (CFRP) laminates is a very challenging issue. Difficulties come from the weak contrast between the thermal properties of constitutive parts, the small thickness of the epoxy joint and also the depth of the bonded interface. The strategy considered in this work is to design a new joint material specially adapted to the NDT detection of bonding defects. Using a numerical model, it is suggested to reinforce the epoxy joint material with conductive boron nitride particles. Experimental investigation of defective assemblies confirms the interest of such approach through a clear improvement of the IRT defect detection capacity.

1. Introduction

If the interest of bonding repair for composites aeronautical elements has been clearly demonstrated, specially regarding mechanical and aerodynamical performances, its wider development is still hampered by some difficulties in assessing their reliability by means of non destructive techniques. For instance review papers of [1–3] compare different assessment techniques for bonded repair (ultrasound, shearography, IRT, etc.) with related advantages and limitations. If ultrasonic methods are for now the most commonly used in aviation industry, IRT associates field investigation and non-contact inspection that provide new attractive solutions. In the case of CFRP laminates, the structural joint between parent and patch parts is generally of same nature as composite matrix (epoxy type). This weak contrast inside the assembly therefore limits the detection capacity of IRT techniques.

Different types of IRT methods exist in literature and can be distinguished by the nature of the excitation used to thermally stimulate the sample, for instance vibro [3], electromagnetic [4], lock-in Ref. [5] or pulsed source [6]. Industrial constraints encourage the development of fully non-contact, easy handling and data processing NDT methods. In this way, authors have recently proposed a specific experimental procedure to improve the capacity of active IRT to detect a bonded interface inside a carbon-epoxy repaired assembly [7]. In this work, a step heating approach is used for exciting the specimen and the thermographic data processing is simply based on the thermal contrast induced on the structure surface. Using this approach now allows to distinguish the specific joint response, at least up to 2.3 mm deep within the laminate. Yet, thermal gradients between different parts of the assembly remain very low. Moreover, in the case of thin bonding defects introduced during repair operation [8,9], heat can transfer across the narrow air gap which makes it even more difficult to detect such kind of heterogeneities.

In addition to such experimental IRT procedure, the strategy considered in this paper is to design the joint material in view of non destructive thermal requirements. Quite similar approach is adopted for X-ray micro-tomography acquisitions through the inclusion of marker particles inside materials to give better contrasts in volume images [10,11]. In the present context, thermal gradients between bonded parts and their defects may be enhanced by modifying the thermal properties of the epoxy joint, specially its thermal conductivity. In this way, the material modification through the introduction of additives in a polymer matrix that was already suggested for several industrial applications

* Corresponding author.
E-mail addresses: matthias.barus@enit.fr (M. Barus), helene.welemane@enit.fr (H. Welemane), valerie.nassiet@enit.fr (V. Nassiet), marie.laetitia.pastor@iut-tarbes.fr (M.L. Pastor), arthur.cantarel@iut-tarbes.fr (A. Cantarel), francis.collombet@iut-tlse3.fr (F. Collombet), laurent.crouzeix@iut-tlse3.fr (L. Crouzeix), yh.grunevald@composites-expertise-solutions.com (Y.H. Grunevald).

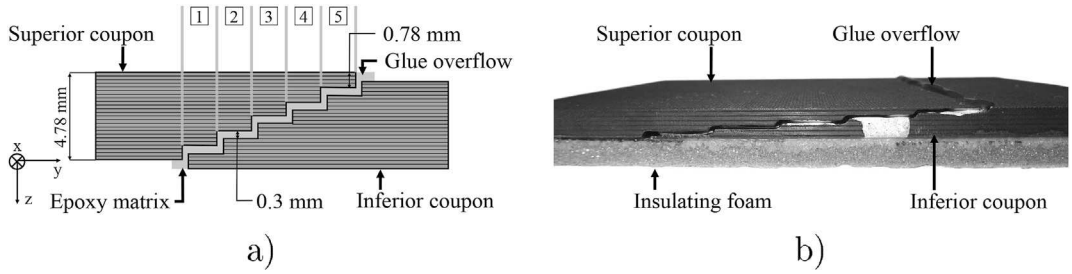

Fig. 1. Lateral view of the study assembly: schematic representation (a), real assembly (b).

[12–14] seems a relevant solution. However, such approach has never been extended to the context of structural health investigation by IRT. The original contribution of this work is thus to define and elaborate an epoxy-based joint material including additives with specific infrared signature that could exacerbate the contrast between virgin and defective zones of internal interfaces.

After the presentation of materials and a short recall of the methodology developed in Ref. [7] (section 1), the influence of the joint thermal behaviour onto the assembly thermal response is studied by means of the numerical model of the thermal problem. The new joint material (global behaviour, relevant additives, volume fraction) will then be designed in order to highlight bonding defects inside the assembly (section 2). Validation of the work will finally be demonstrated through the experimental study of defective bonded assemblies by active IRT, for both epoxy matrix and loaded epoxy joint material (section 3).

2. Materials and active IRT procedure

The studied material is a $[0/90/0]_6$ laminated composite composed of HEXPLY® M10R/38%/UD150/CHS made by HEXCEL® with TORAYCA® T300 carbon fibers (4.7 mm global thickness, transversely isotropic ply, 0∘ axis corresponds to Y axis). A step lap assembly accounting for repair configuration has been considered which allows to investigate the structural joint at different depths [3]. Two composite elementary coupons are bonded with an epoxy glue (resin LY5052, hardener HY5052 from HUNTSMAN®) called subsequently *epoxy matrix* (Fig. 1). Thermo-physical properties of materials are given in Table 1.

The active IRT procedure developed by authors [7] uses a specific experimental device specially designed to control tests conditions (Fig. 2). Precisely, all elements of the thermal bench are accurately positioned into rigid metallic profiles to define the geometry and position of the heated area. Thermal stimulation of coupons is conducted using a halogen lamp (maximum power of 1000W) associated with an optical set-up to deliver a quasi homogeneous heating inside the (elliptic) thermally stressed area. Furthermore, environmental effects (like the light reflexions) are minimized by painting the studied surfaces in mat black (005641 from JELT®) and by measuring the surface temperature variations in relative temperature $\Delta T(t) = T(t) - T_0(t = 0)$. Regarding boundary conditions, all coupons are sticked onto an insulating foam (Airex C70 by SICOMIN®) with an epoxy glue (resin SR1126 and hardener SD8205 from SICOMIN®) that insulates the sample back face. Thermal acquisition is finally performed using a FLIR® Titanium retrofitted camera (InSb sensors, thermal resolution of 25 mK, focal plane of 320 × 256 pixels) associated with Altair software. Note that the detailed design of the test procedure and choice justification can be found in Ref. [7].

The representation of heat transfer inside the material can be modelled using the classical thermodynamics background [15]. Let consider V the volume of the studied assembly. $T = T(x, y, z, t)$ denotes the local temperature of point $M(x, y, z)$ of V at time t. Combination of thermodynamics principles with Fourier conduction law leads to the well-known expression of the local heat equation (without internal sources):

$$\rho C_p \frac{\partial T}{\partial t} - \vec{\nabla} \cdot \left(\lambda \vec{\nabla}\, T\right) = 0,\ \forall M \in V \tag{1}$$

with ρ the material density, C_p the specific heat and λ the thermal conductivity tensor at point M. Heat flow on the elliptical impacted area S_l (dimensions $a = 65$mm and $b = 72$mm) is assumed to be homogeneous. Its intensity ϕ has been identified on reference materials [7] and evolves in form of a step of 10s (beginning at $t = 2$s, end at $t = 12$s, see Fig. 3). In view of low temperature variations induced within the material, convective and radiative phenomena are neglected and the initial state is defined by the ambient temperature T_{amb} within the laboratory. Spatial and temporal boundary conditions for the problem can thus be summarized by:

$$\begin{cases} n \cdot \left(\lambda \vec{\nabla}\, T\right) = \phi, \forall M \in S_l\ ;\ n \cdot \left(\lambda \vec{\nabla}\, T\right) = 0, \forall M \in S - S_l \\ T(x, y, z, t = 0) = T_0 = T_{amb}, \forall M \in V \end{cases} \tag{2}$$

with S the outer surface of V, n the outward unit normal to S. In following parts, the transient thermal response of materials deduced from Eq. (1)

Table 1
Thermo-physical properties used for simulations (λ_a and λ_t : axial and transverse conductivity). Note that (a) and (c) data are estimations while others have been determined in related references.

		P [ρ kg m^{-3}]	C_p [J kg^{-1}K^{-1}]	λ [W m^{-1}K^{-1}]
	Composite ply (0°) [7]	1550	883	$\lambda_a = 3.05$ $\lambda_t = 0.51$
	Epoxy matrix [7]	1172	1317	0.226
	Air [23]	1.177	1007	0.0261
(a)	Insulating behaviour	1172	1317	0.045
	Conductive behaviour	1172	1317	1.13
(b)	Alumina [19,24]	3970	880	35
	Boron nitride [14]	2280	1610	300
(c)	60% Al_2O_3 loaded epoxy	2850	1055	1.2
	60% BN loaded epoxy	1837	1493	16.9

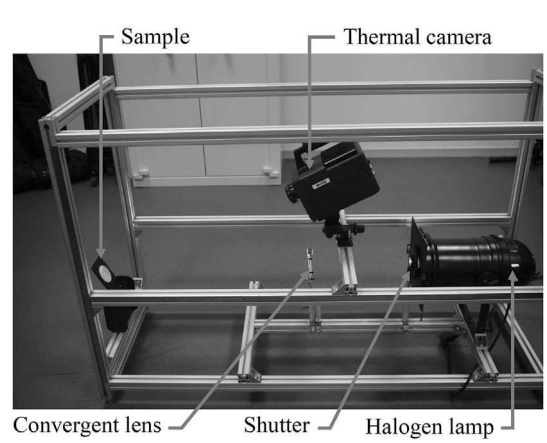

Fig. 2. Specific thermal device.

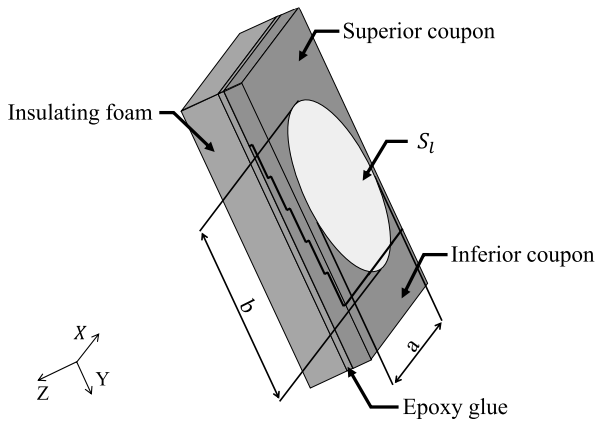

Fig. 3. Schematic representation of the thermal problem.

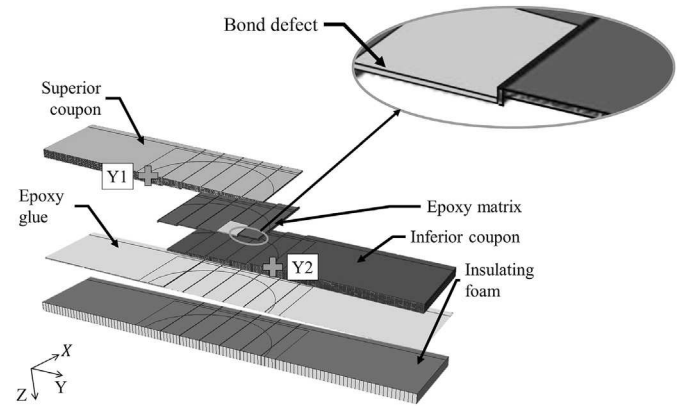

Fig. 5. Constitutive parts of the FE model with bonding defect (points Y1 and Y2 correspond to the vertical limits of the heated area).

and boundary conditions (2) is numerically solved by finite element method using Abaqus software. Detailed information regarding numerical aspects can be found in Ref. [7], specially the demonstration of the good agreement between numerical and experimental thermal fields.

Note finally that some next results, both experimental and simulated, will be based upon a post-processing in order to highlight the thermal response of the adhesive joint and then help in differentiating its specific response. Precisely, the *relative temperature* $\Delta T_2(t) = \Delta T_{ass}(t) - \Delta T_{mono}(t)$ is obtained by subtracting from the thermal field variation $\Delta T_{ass}(t)$ of the repaired assembly the thermal field variation $\Delta T_{mono}(t)$ obtained at the same time t for an equivalent but monolithic (non repaired) sample (same material and same geometry, Fig. 4). Such procedure makes it possible to remove lens edge effects and allows to access to the thermal response of the three shallowest steps (2.3 mm depth within the laminate). Note also that the ΔT_2 evolution highlights in all cases the thermal peak induced by the glue overflow (located between step nº5 and point Y2 on ΔT_2 plots).

3. Joint material design

The objective of this section is to define a new epoxy-based joint material whose additives would improve the detection of bonding defects by the active IRT procedure described before. Given the performance of the model developed before, this numerical tool was used to guide design choices.

3.1. Definition of the joint thermal behaviour

Though many parameters can affect the joint thermal response, the assumption that the thermal conductivity is a significant one can however be taken [16]. Accordingly, one has considered in simulations an insulating (respectively conductive) behaviour compared to the epoxy matrix obtained by dividing (resp. multiplying) its thermal conductivity by a factor five. Density and specific heat are assumed to remain the same. Moreover, a bonding defect with a width of 20 mm has been numerically created at the second bonding interface (step 4 at a depth of 1.56 mm, Figs. 1 and 5) by replacing the joint properties by those of the air at 20 °C (Table 1-a). Note also that results for adhesive bonded assemblies without defect (denoted *virgin*) are also provided as a reference.

Let focus on the end of the heating phase ($t = 12$s) for which thermal gradients are the most important. Due to its natural insulating behaviour, the epoxy matrix acts as a thermal barrier and generates a local temperature elevation ΔT_{ass} higher than that obtained for the monolithic composite ΔT_{mono}, so $\Delta T_2 \geq 0$, specially where the joint is shallowest [7] (red area on the left hand side of Fig. 6-a, corresponding to the step nº5 and close to the point Y2). Using a more insulating joint material increases such tendency. On the contrary, the conductivity of the joint in the more conductive scenario is greater than the transverse conductivity of the composite ply, leading to a better heat conduction along the X direction (along width of the steps) and along Z direction (in the thickness of the assembly). In that case, $\Delta T_{ass} \leq \Delta T_{mono}$, leading to a negative relative temperature ($\Delta T_2 \leq 0$, on the right hand side of Fig. 6-a). Since air captured inside the bonding defect exhibits an insulating thermal behaviour, the local temperature variations induced by this kind of defect are then covered by those of epoxy matrix (which has also an insulating behaviour compared to laminated coupons). Which such configuration, the defect is hidden and IRT may be unreliable to detect it. It is thus more relevant to use a more conductive behaviour for the joint as disturbances generated by the joint interface and bonding defect are of opposite

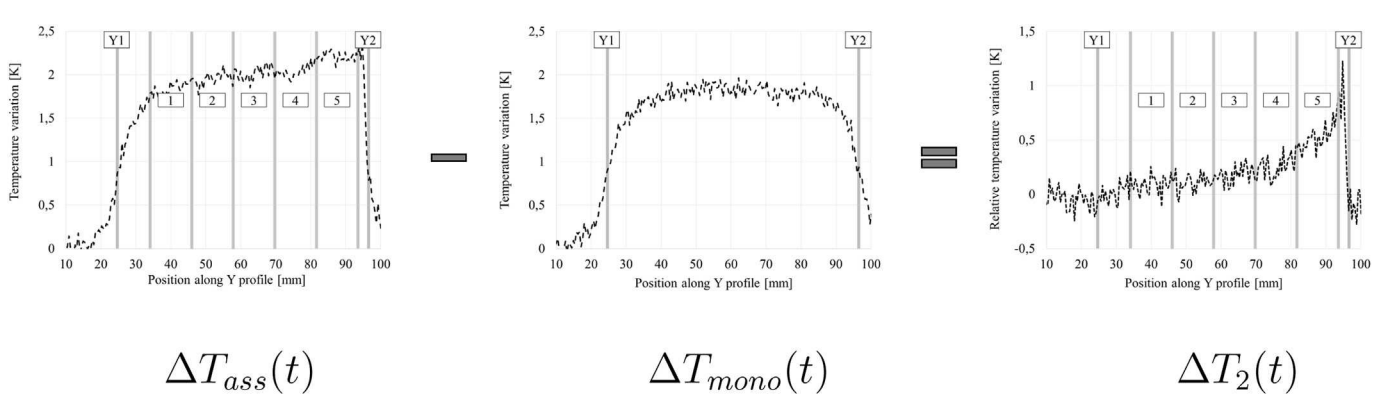

Fig. 4. Example of $\Delta T_2(t)$ post-processing: case of an insulating joint material.

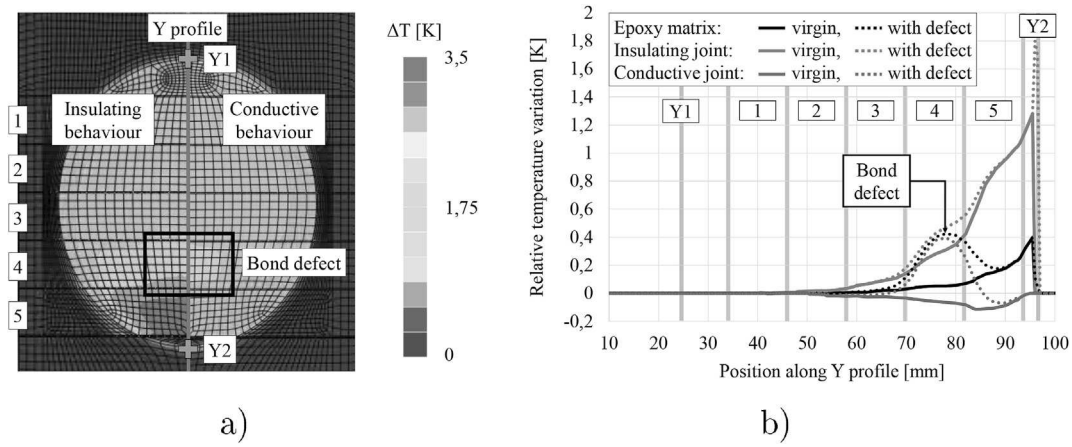

Fig. 6. Influence of the joint thermal behaviour: simulated surface temperature variation ΔT (a) (left hand side: insulating behaviour, right hand side: conductive behaviour), relative temperature variation ΔT_2 along the Y profile (b) at $t = 12s$.

nature. Simulation of Fig. 6-b clearly illustrates such interest in the event of a defect.

3.2. Choice of conductive additives

Two types of conductive additives commonly used to modify the thermal properties of materials were considered and microstructurally examined by Scanning Electron Microscopy (SEM):

- Alumina ALM-41-01 from SUMITUMO® (aluminum oxide, Al_2O_3, [17–19]), whose particles are spherical with an average diameter of 2 μm (Fig. 7-a),
- Boron nitride CTP8 from SAINT-GOBAIN® (BN, [13,14,20]), in form of platelets particles with an average size of 8 μm (Fig. 7-b).

Properties of these materials are described in Table 1-b. In order to make the best choice among them, one proposes to simulate the thermal response obtained with a composite joint made of epoxy matrix and each of these additives. It is thus necessary to estimate its global thermo-physical properties according to the constituents ones. In considering a Representative Elementary Volume (REV) of the joint with a size upper than those of the particles, numerous schemes aim at predicting the effective behaviour of such composite material. In view of the spherical shape of alumina particles (see Ref. [14]), the law of Maxwell-Garnet appears to be suitable for the estimation of the effective thermal conductivity λ_{eq} for the Al_2O_3 loaded epoxy:

$$\lambda_{eq} = \lambda_m \left[1 + \frac{3f \frac{\lambda_a - \lambda_m}{\lambda_a + 2\lambda_m}}{1 - f\left(\frac{\lambda_a - \lambda_m}{\lambda_a + 2\lambda_m}\right)} \right] \tag{3}$$

while the logarithmic of Lichtenecker seems more relevant in case of platelet boron nitride additives:

$$\ln \lambda_{eq} = (1 - f) \ln \lambda_m + f \ln \lambda_a \tag{4}$$

In equations (3) and (4), λ_m (respectively λ_a) denotes the thermal conductivity of the epoxy matrix (resp. of additives) for a volume fraction f of additives, effective density and specific heat being deduced by the classical mixture law. Note finally that simulations have been performed in both cases for a volume fraction $f = 60\%$ which corresponds to the theoretical maximum rate guaranteeing an homogeneous mixing of constituents [21]. Table 1-c gives related effective properties of the composite joint used for simulations.

The influence of both additive inclusions inside the epoxy matrix is shown on Fig. 8. The relative temperature variations ΔT_2 along the Y profile confirms that the use of those particles leads to relative temperature variations $\Delta T_2 \leq 0$ in both cases. However, the responses of alumina and boron nitride loaded epoxy are clearly distinct, with a higher amplitude obtained for BN. For instance, regarding the step n°5 in the case without defect, the relative temperature variations ΔT_2 obtained for BN loaded epoxy joint is almost twice that provided with alumina additives. These results are directly linked to the high thermal conductivity of boron nitride material and of the associated loaded joint. As

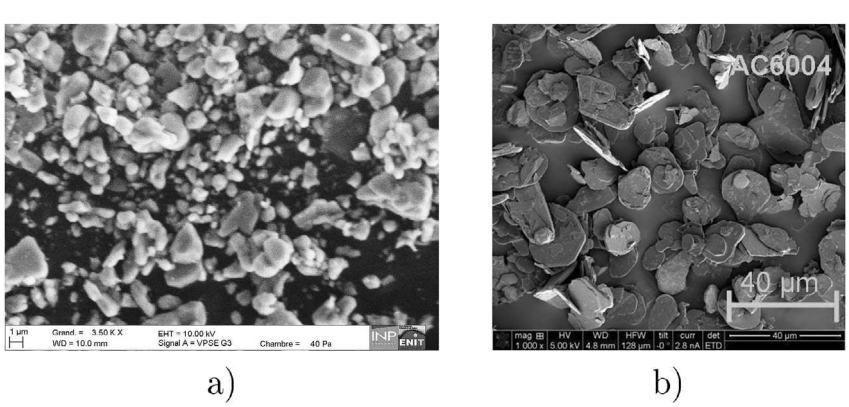

Fig. 7. SEM micrograph of studied particles: alumina (a), boron nitride (b).

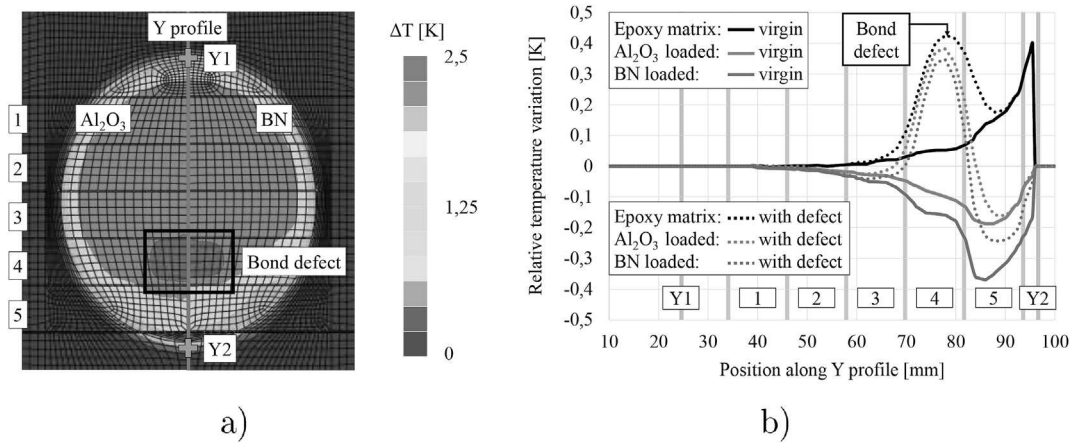

Fig. 8. Influence of additives inside the loaded epoxy matrix: simulated surface temperature variation ΔT (a) (left hand side: Al_2O_3 loaded epoxy, right hand side: BN loaded epoxy), relative temperature variation ΔT_2 along the Y profile (b) at $t = 12$s.

assumed before, the thermal conductivity thus essentially governs heat flow transmission in the present context. In the presence of a bond defect, the contrast with the virgin assembly is consequently much more important with boron nitride additives, which helps in addressing the detection problem. Accordingly, BN particles have been selected in what follows to elaborate the new joint material.

3.3. Elaboration and characterization of the BN loaded epoxy

The inclusion of boron nitride inside the epoxy matrix requires a special attention during the elaboration process otherwise numerous voids would lead to a foam-type structure (Fig. 9-a). The aim of such procedure is then to ensure the most complete outflow of air bubbles encapsulated between platelet particles and the most homogeneous blending of constituents. In addition, beyond a volume fraction $f = 8\%$ of boron nitride, the BN loaded epoxy blend exhibits a so important viscosity that it is required to use acetone to improve its solubility [14]. Acetone being volatile at 20 °C, it is naturally removed during the air outflow done under vacuum. Moreover, possible traces of acetone do not interfere with the improvement of thermal conductivity, they may even increases it [22]. Following these recommendations allows to optimize the elaboration phase (Fig. 9-b) with an homogeneous repartition of particles and almost no voids (see SEM observation on Fig. 9-c). Yet, beyond an additives volume fraction of $f = 18\%$, the blend viscosity prevents the air outflow after curing, even with acetone, such volume fraction will thus be considered hereafter.

The introduction of boron nitride particles into the epoxy matrix allows a significant enhancement of the conductivity. Indeed, thermal measurement using HOT-DISK® TPS2500S gives $\lambda = 0.79 \mathrm{Wm^{-1}K^{-1}}$ for the new joint material (which stands in agreement with the Lichtenecker model), that is an increase of 250% compared to epoxy matrix. It should be noted that the density and the specific heat are little affected by the use of BN additives (respective increase of 14% and 3% compare to epoxy matrix).

4. Infrared investigation of assemblies bonded with the loaded joint

The geometry of studied assemblies remains as before (Fig. 1) and the 0.3 mm thickness joint was calibrated with sheets of Teflon paper placed on the two deepest steps (nº1 and 2). The inferior and superior elementary coupons of both assemblies come from a single layup and were machined at the same time by abrasive water jet. Once the BN loaded epoxy (or epoxy matrix) is applied on the three shallowest steps of the inferior coupon (nº3, 4 and 5), the superior coupon is put down on the assembly and the assembly is hold during the curing process (15 min at 80 °C). Accordingly, one can assume a constant thickness of the joint along the bond line. Moreover, as the duration and amplitude of the thermal load do not allow the heat flow to reach the two deepest steps, the thermal surface field is therefore not affected by the Teflon paper.

The active IRT procedure was applied on defective assemblies including two partially bonded areas accounting for bonding defects (Fig. 10):

- a small zone located at the border of the step nº5 (depth of 0.78 mm), denoted defect nº1,
- a wider one covering nearly all the central part of the step nº4 (depth of 1.54 mm), called defect nº2.

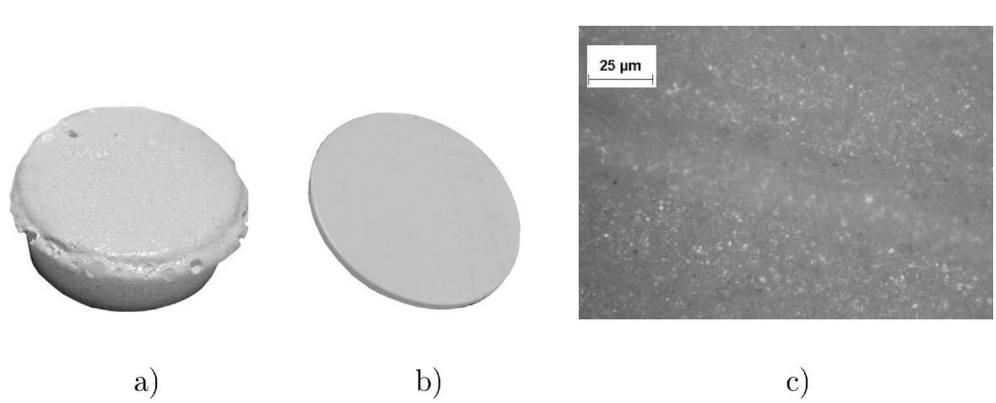

Fig. 9. Elaboration process of BN loaded epoxy: non optimized mix (a), optimized mix with $f = 18\%$ (b) and related SEM micrograph (c).

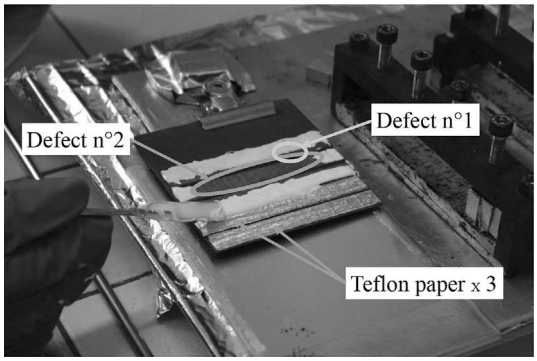

Fig. 10. Preparation of the tested assembly.

In order to highlight the contribution of the new joint material, such preparation has been done for assemblies with both epoxy matrix and BN loaded epoxy.

Using the epoxy matrix does not allow to distinguish the defects response among the thermal results for assemblies, even on the relative temperature variation field ΔT_2 (Fig. 11-a). Infrared investigation is thus very limited in that case. On the contrary, Fig. 11-b clearly illustrates the ability of the new joint material to capture the two bonding defects located at different depths. Thermal evolutions along profiles passing through each defect (yellow profile for defect nº1 and orange profile for defect nº2) confirm these conclusions. Moreover, one can identify with the loaded epoxy the spatial location of defect quite precisely. Indeed, the related maximum elevation of ΔT_2 on the specimen surface appears in the corresponding zone of defective interfaces, respectively step nº5 for defect nº1 obtained after 5s of heating (Fig. 11-c), and step nº4 for defect nº2 after 10s of heating (Fig. 11-d). These ΔT_2 elevations are induced by defects whereas thermal peaks at around Y = 95 mm on Fig. 11-c and d correspond to the glue overflow at the sample surface denoted on Fig. 1 (precisely these latter values differ between Fig. 11-c and d according to the heating time and the position of the Y profile in the heated area). In agreement with numerical simulations, the introduction of boron nitride additives seems thus a relevant design option to improve the detection capacity of infrared techniques.

5. Conclusions

The original approach proposed in this study, based on material design, brings a clear contribution to experimental mechanics and specially to the non destructive testing of bonded interfaces inside composite materials. Using a numerical model of the thermal problem has led to the definition of a new epoxy-based joint material including additives that enhances the IRT detection capacity. In the present study, experimental results on defective bonded assemblies show the significant interest of the introduction of boron nitride particles into the epoxy matrix to capture bonding defects. It should be noted that this certainly can be further improved by optimizing the elaboration process (leading to higher volume fraction or using more efficient types of additives) and the thermographic data processing to better highlight defect (using filtering procedures for instance). Moreover, the complete validation of such strategy for the analysis of engineering interfaces now requires the characterization of the influence of additives inclusion on the matrix mechanical behaviour and the definition of the detection limit size of the technique.

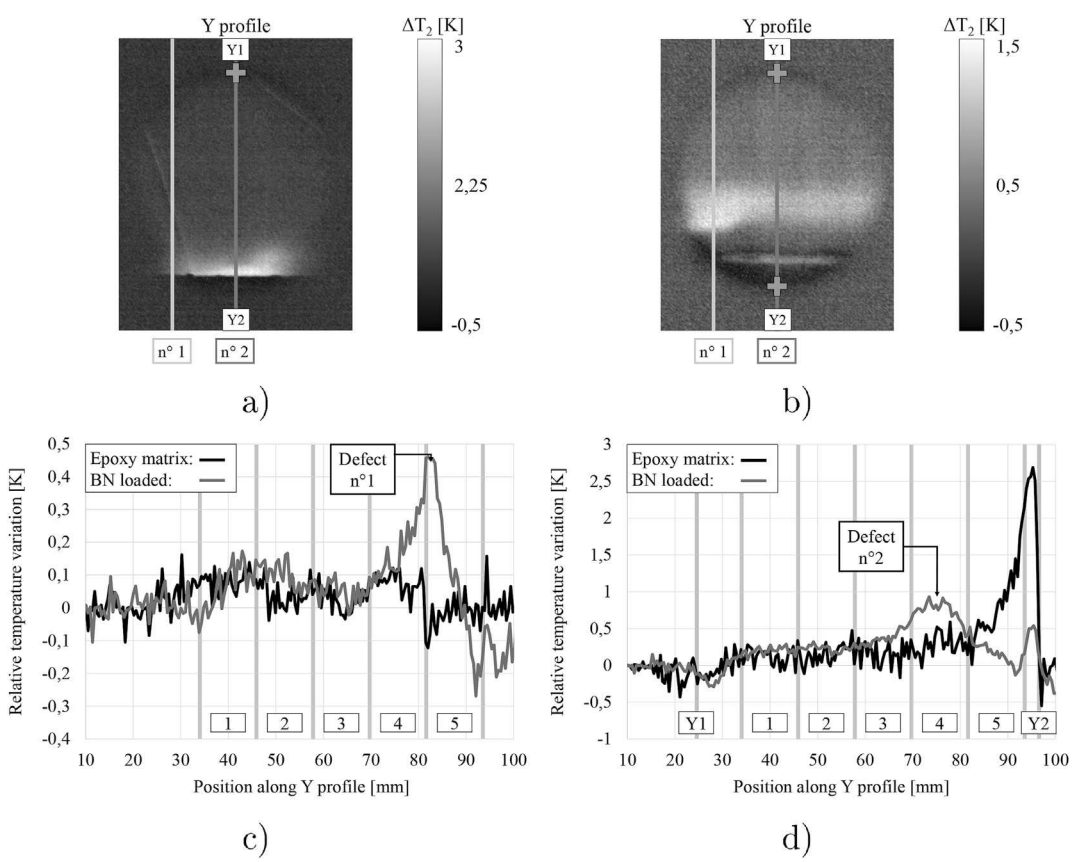

Fig. 11. Experimental relative temperature variation ΔT_2 for defective bonded assemblies according to the joint material: ΔT_2 fields for epoxy matrix (a) and BN loaded epoxy (b), ΔT_2 evolution along yellow Y profile (passing through defect nº1) at $t = 7$s (c) and along orange Y profile (passing through defect nº2) at $t = 12$s (d).

Acknowledgements

The authors would like to show their gratitude to the French Midi-Pyrénées Region who supported this research project.

References

[1] Adams RD. Non destructive testing. In: Da Silva LFM, Öchsner A, Adams RD, editors. Handbook of adhesion technology. Berlin: Spring-Verlag; 2011. p. 1049–69.
[2] Adams RD, Drinkwater BW. Nondestructive testing of adhesively-bonded joints. NDT E Int 1997;30:93–8.
[3] Baker A, Gunnion JA, Wang J. On the certification of bonded repairs to primary composite aircraft components. J Adhes 2015;91:4–38.
[4] Gao B, Woo W, Tian G. Electromagnetic thermography nondestructive evaluation: physics-based modeling and pattern mining. Sci Rep 2016;6:25480. https://doi.org/10.1038/srep25480.
[5] Palumbo D, Galietti U. Damage investigation in composite materials by means of new thermal data processing. Strain 2016;52:276–85.
[6] Lopez F, Ibarra-Castanedo C, De Paulo Nicolau V, Maldague X. Optimization of pulsed thermography inspection by partial least-squares regression. NDT E Int 2014;66:128–38.
[7] Barus M, Welemane H, Collombet F, Pastor ML, Cantarel A, Crouzeix L, et al. Bonded repair issues for composites: an investigation approach based on infrared thermography. NDT E Int 2017;85:27–33.
[8] Adams RD. The non destructive evaluation of bonded structures. Constr Build Mater 1990;4:3–8.
[9] Yan D, Drinkwater BW, Neild SA. Measurement of the ultrasonic nonlinearity of kissing bonds in adhesive joints. NDT E Int 2009;42:459–66.
[10] Germaneau A, Doumalin P, Dupré JC. Comparison between X-ray micro-computed tomography and optical scanning tomography for full 3D strain measurement by digital volume correlation. NDT E Int 2008;41:407–15.
[11] Nielsen SF, Poulsen HF, Beckmann F, Thorning C, Wert JA. Measurements of plastic displacement gradient components in three dimensions using marker particles and synchrotron X-ray absorption microtomography. Acta Mater 2003;51:2407–15.
[12] Juárez D, Ferrand S, Fenollar O, Fombuena V, Balart R. Improvement of thermal inertia of styrene-ethylene/butylene-styrene (SEBS) polymers by addition of microencapsulated phase change materials (PCMs). Eur Polym J 2011;47:153–61.
[13] Zhou W, Qi S, An Q, Zhao H, Liu N. Thermal conductivity of boron nitride reinforced polyethylene composites. Mater Res Bull 2007;42:1863–73.
[14] Zhu B, Ma J, Wu J, Yung KC, Xie CS. Study on the properties of the epoxy-matrix composites filled with thermally conductive AlN and BN ceramic particles. J Appl Polym Sci 2010;118:2754–64.
[15] Germain P, Nguyen QS, Suquet P. Continuum thermodynamics. J Appl Mech 1983; 50:1010–20.
[16] Li J, Xue P, Ding W, Han J, Sun G. Micro-encapsulated paraffin/high-density polyethylene/wood flour composite as form-stable phase change material for thermal energy storage. Sol Energ Mat Sol C 2009;93:1761–7.
[17] Das S, Putra N, Roetzel W. Temperature dependence of thermal conductivity enhancement for nanofluids. Am Soc Mech Eng 2003;125:567–74.
[18] Xie H, Wang J, Xi T, Liu Y, Ai F, Wu Q. Thermal conductivity enhancement of suspensions containing nanosized alumina particles. J Appl Phys 2002;91:4568–72.
[19] Zhou W, Qi S, Tu C, Zhao H, Wang C, Kou J. Effect of the particle size of Al_2O_3 on the properties of filled heat-conductive silicone rubber. J Appl Polym Sci 2007;104: 1312–8.
[20] Gaska K, Rybak A, Kapusta C, Sekula R, Siwek A. A study of thermal conductivity of boron-nitride epoxy-matrix composite. In: Proceeding of EECM-15 conference. Venice; June, 2012.
[21] Lee GW, Park M, Kim J, Lee JI, Yoon HG. Enhanced thermal conductivity of polymer composites filled with hybrid filler. Compos Part A Appl S 2006;37: 727–34.
[22] Xu Y, Chung DDL. Increasing the thermal conductivity of boron nitride and aluminum nitride particle epoxy-matrix composites by particle surface treatments. Compos Interface 2000;7:243–56.
[23] Marchio D, Reboux P. Introduction aux transferts thermiques. Paris: Mines ParisTech Les Presses "Les cours de l'école des mines"; 2008. 210pp.
[24] Ceramic materials and ceramic components. June, 2017. http://accuratus.com/alumox.html.